Quantum Confinement-Controlled Exchange Coupling in Manganese(II)-Doped CdSe Two-Dimensional Quantum Well Nanoribbons

ARTICLE *in* NANO LETTERS · SEPTEMBER 2012

Impact Factor: 13.59 · DOI: 10.1021/nl302639k · Source: PubMed

7 AUTHORS, INCLUDING:

Rachel Fainblat
Seoul National University
5 PUBLICATIONS **11** CITATIONS
SEE PROFILE

Julia Frohleiks
University of Duisburg-Essen
2 PUBLICATIONS **13** CITATIONS
SEE PROFILE

Franziska Muckel
University of Duisburg-Essen
4 PUBLICATIONS **29** CITATIONS
SEE PROFILE

Jiwoong Yang
Seoul National University
9 PUBLICATIONS **57** CITATIONS
SEE PROFILE

Supporting Information

Quantum Confinement-controlled Exchange Coupling in Manganese(II)-doped CdSe Two-dimensional Quantum Well Nanoribbons

Rachel Fainblat[1,], Julia Frohleiks[1], Franziska Muckel[1], Jung Ho Yu[2], Jiwoong Yang[2], Taeghwan Hyeon[2], and Gerd Bacher[1]*

[1] *Werkstoffe der Elektrotechnik and CeNIDE, Universität Duisburg-Essen, Bismarckstraße 81, 47057 Duisburg, Germany*

[2] *School of Chemical and Biological Engineering, Seoul National University, Seoul 151-744, Korea*

* E-mail: rachel.fainblat-padua@uni-due.de

Sample preparation:

The CdSe:Mn^{2+} two-dimensional quantum well nanoribbons were synthesized from the Lewis acid-base reaction of $CdCl_2$ and $MnCl_2$ with octylammonium selenocarbamate in octylamine coordinating solvent. Initial relative $MnCl_2$ concentrations of 5.0%, 10.0% and 15.0% with respect to $CdCl_2$ were used for the synthesis. During the synthesis, the reacting solution color becomes turbid-white at 70 ^oC, which is an indicative of UV-absorbing $(CdSe)_{13}$ cluster formation. The Mn^{2+}-doping into the clusters can be visualized by orange-red photoluminescence from the UV photo-excited reacting solution. Finally, during the aging process for 24~48 hrs, the solution color changes from white to yellow, indicating that the CdSe:Mn^{2+} quantum well nanoribbons were produced from the assembly of $(CdSe)_{13}$:Mn^{2+} clusters. The doped Mn concentration was measured using inductively coupled plasma-atomic emission spectroscopy (ICP-AES). Before the determination of the incorporated Mn^{2+} ions, the nanoribbons were repeatedly washed with pyridine for five times to remove not lattice-incorporated, but surface-bound Mn^{2+} ions on the nanoribbon surface. The Mn^{2+} ions inside CdSe nanoribbons determined by the method are 4.0(±0.4)%, 8.3(±0.5)% and 9.9 (±0.2)% compared to the initial $MnCl_2$ concentration of 5.0%, 10.0% and 15%.

For the magneto-optical spectroscopy, a few drops of oleylamine or octylamine were added to the CdSe:Mn^{2+} nanoribbons in chloroform solution. This step allows uniform thin-film formation by spin-casting or drop-casting, which was found out to be critical for resolving light hole and heavy hole splitting in the absorption spectra.

Optical sample characterization:

The drop-casted CdSe nanoribbon thin-films were characterized by UV-VIS absorption spectroscopy and photoluminescence (PL) spectroscopy. The UV-VIS spectra were obtained using a Shimadzu UV-2550 spectrometer. Fig S1 depicts the absorption spectra of an undoped sample and three samples of different manganese concentration. Three excitonic transitions can be identified, the heavy hole (hh-X), light hole (lh-X) and split off (so-X) excitons, which are marked with different colors. The incorporation of manganese into the nanoribbons results in a clear and systematic energy shift of the bandgap, both for the heavy hole and the light hole exciton transition, which can be seen in the inset of Fig S1.

The PL was measured using a frequency doubled Ti:Sa laser with a wavelength of 400 nm as an excitation source and a monochromator with a LN_2 cooled CCD camera for detection. The samples were cooled down to 5 K by a continuous flow optical microscope cryostat Janis ST-300-MS. The emission spectra of both, undoped and 8.3% manganese doped nanoribbons can be seen on Fig S2. The black curve represents the sharp emission spectrum generated by the excitonic bandgap emission of the undoped sample. In contrast, the doped counterpart exhibits a red-shifted emission spectrum arising from the internal $4T_1 \rightarrow 6A_1$ manganese transition.

These results demonstrate the successful doping of the magnetic ions into the host semiconductor matrix.

Crystallographic sample characterization:

Powder X-ray diffraction patterns were obtained with a Rigaku D/Max-3C diffractometer equipped with a rotating anode and a Cu Kα source (λ = 0.15418 nm) in order to analyze the variation of the lattice parameters compared to bulk.The lattice parameters calculated from XRD of CdSe nanoribbons (undoped) were a = 4.19 Å and c = 6.95 Å.[1] Compared to those of bulk CdSe (a = 4.299 Å and c = 7.010 Å), lattice contractions of Δa = 2.53 % and Δc = 0.85 % occurred. In contrast to the bulk crystals, in which the lattice parameters are reduced by Mn ion doping, in the case of CdSe nanoribbons, a lattice expansion occurs by the Mn ion doping. In the following table, the corresponding numbers are given.

Sample	a-Axis	c-Axis
CdSe Nanoribbons	4.1876(0.0022)	6.9592(0.0085)
4.0 %-doped CdSe:Mn NRs	4.1918(0.0015)	7.0128(0.0161)
8.3 %-doped CdSe:Mn NRs	4.1986(0.0013)	7.0288(0.0185)
9.9 %-doped CdSe:Mn NRs	4.2014(0.0022)	7.0516 (0.0256)
Bulk CdSe	4.299	7.01~7.02

The slight difference of the lattice constants and the local relaxation in nanoribbons might contribute to the variation of the exchange constants as compared to bulk. Although it is challenging to quantitatively account for this effect, the huge quantum confinement energy (which is on the order of about 1 eV in our nanoribbons) should be considered. Thus, the exchange constants will be affected by the quantum confinement rather than by the strain or local relaxation.

Impact of the sample geometry on the transition probabilities:

Assuming a thin nanoribbon layer on a substrate with the *c*-axis predominantly oriented along the substrate surface (see Fig. S3), we may consider two limiting cases I (quantization axis parallel to the surface) and III (quantization axis perpendicular to the surface) (see Fig. 3a). According to the selection rules for a quantum well[4] the probability of the hh excitonic transition in case III is 1/2 for both light polarization parallel and perpendicular to the long axis of the nanoribbon. However, due to the wurtzite geometry, the heavy hole transition is forbidden if the incoming light is polarized parallel to the *c*-axis. Thus, the hh-X can only be excited if the polarization is perpendicular to the *c*-axis in case III. The lh excitonic transition can be generated by both, light polarized perpendicular and parallel to the *c*-axis with an equivalent oscillator strength (1/6 for each case). Therefore, in case III, the transition probability will be 1/2 and 1/3 for the hh-exciton and lh-exciton, respectively.

In contrast, for case I, the quantum confinement results for the hh-exciton in a transition probability of 1/2, if the light is polarized along the long axis of the nanoribbons and 0, if the light polarization is perpendicular to this axis. Considering in

addition the wurtzite structure, where the optical excitation of the hh-exciton is forbidden for a polarization parallel to the *c*-axis[5], it is obvious that the optical excitation of the hh excitonic transition is not possible in this geometry. Regarding the lh-exciton, the transition probabilities are 1/6 and 2/3 for polarized excitation along and perpendicular to the *c*-axis, respectively. For the sake of completeness, case II has to be considered, representing a certain angle φ between the quantization axis *z* and the substrate surface. The relative oscillator strength for both, hh-X and lh-X transitions can be easily calculated for each angle φ according to the arguments given above.

In order to quantify the error of the determination of the exchange constants due to a certain angle between *c*-axis and sample surface, we assumed a finite angle between the *c*-axis and the substrate surface statistically varying from 0° to 10° (which seems to be reasonable taking into account the length of few micrometers of the nanoribbons and the film thickness of less than 300 nm). We obtain $\overline{N_0\alpha} = -0.01 \pm 0.01\ eV$ and $\overline{N_0\beta} = -1.31\ \pm 0.12\ eV$, which within the error bars agree with the values obtained assuming that the *c*-axis and the substrate surface are exactly parallel. Therefore, we can affirm that small deviations of the angle between the *c*-axis of the nanoribbons and substrate surface do not significantly alter the conclusions given.

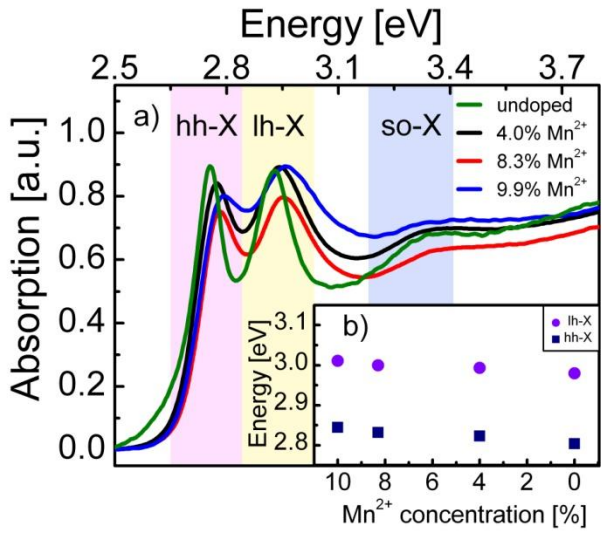

FIG. S1. (a) Absorption spectra of undoped CdSe nanoribbons compared with nanoribbons doped with 4.0(±0.4)%, 8.3(±0.5)% and 9.9(±0.2)% of manganese at room temperature. The heavy-hole (hh-X), light-hole (lh-X) and split-off (so-X) excitonic transitions can be spectrally separated. (b) Peak energy of the absorption spectrum for the hh-X and lh-X excitonic transitions versus doping concentration.

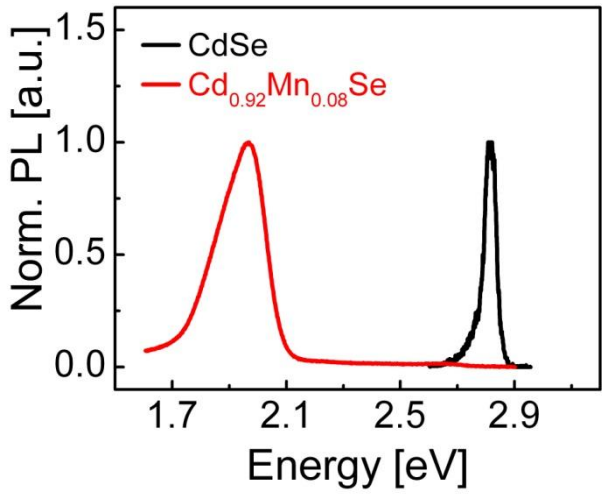

FIG. S2. Normalized photoluminescence spectra of undoped (black) and 8.3% manganese doped (red) CdSe nanoribbons at 5K.

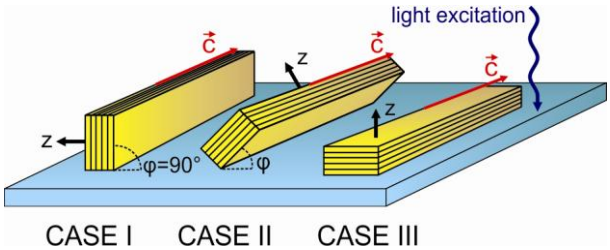

FIG. S3. Different geometries of the nanoribbons indicating the orientation between quantization axis (*z*), *c*-axis, and light excitation.

References:

(1) Joo, J.; Son, J. S.; Kwon, S. G.; Yu, J. H.; Hyeon T. *J. Am. Chem. Soc*. **2006,** *128*, 5632.

(2) Droubay, T. C.; Kaspar, T. C.; Kaspar, B. P.; Chambers, S. A. *Phys. Rev. B*, **2009**, *79*, 075324.

(3) Yu J. H.; Liu X.; Kweon K.E.; Joo J.; Park J.; Ko K.T.; Lee D.W.; Shen S.; Tivakornsasithorn K.; Son J.S.; Park J.H.; Kim Y.W.; Hwang G.S.; Dobrowolska M.; Furdyna J.K.; Hyeon T. *Nat. Mater.* **2010**, *9*, 47-53.

(4) Grundmann, M. *The Physics of Semiconductors*, Springer: Berlin, **2010.**

(5) Gutsche, E.; Jahne, E. *Phys. Status Solidi B* **1967**, *19*, 923-832.